Robust Long-Term Predictive Adaptive Video Streaming Under Wireless Network Uncertainties

Ramy Atawia, *Member, IEEE*, Hossam S. Hassanein, *Fellow, IEEE*, and Aboelmagd Noureldin, *Senior Member, IEEE*

***Abstract*— Recent research on predictive video delivery promised optimal resource utilization and quality of service (QoS) satisfaction to both dynamic adaptive streaming over HTTP (DASH) providers and mobile users. These gains were attained while presuming an idealistic environment with perfect predictions. Thus, a robust QoS-aware *predictive*-DASH (P-DASH) is of paramount importance to handling the practical uncertainty implied in predicted information. In this paper, we propose a *stochastic* QoS-aware *robust predictive*-DASH (RP-DASH) scheme over future wireless networks that takes into account imperfect rate predictions. The objective is to achieve *long-term quality fairness* among the DASH users while capping the probability of service degradation by an operator predefined level. A deterministic formulation is then obtained using the scenario approximation, which adopts the probability density function (PDF) of predicted rates. A linear conservative approximation is introduced to provide an NP-complete formulation, which can be optimized by commercial solvers. Since exact PDF might not be available, Gaussian approximation is adopted by the introduced scheme to provide a closed form less complexity formulation. To support real-time implementations, a guided heuristic algorithm is devised to obtain near-optimal resource allocations and quality selections, while satisfying the predefined QoS level. Previous non-robust P-DASH schemes are evaluated in this paper, while considering typical error models in predicted rates. Such schemes resulted in increased QoS and the quality of experience degradations with the network load, which was avoided by the introduced RP-DASH. Results further revealed the ability of RP-DASH to reach optimal and fair QoS satisfactions.**

***Index Terms*— Channel state information, radio access networks, resource management, robustness, video.**

I. Introduction

MORE than 75% of the global mobile data traffic is expected to be video content in 2020 [1]. This predicted increase is almost fourfold compared to the other internet applications such as browsing, gaming and e-mails. Such growth is driven by the ongoing rapid development of both the mobile devices and the adaptive dynamic streaming protocols that enhance the user's experience under varying channel conditions [2], [3]. Dynamic Adaptive Streaming over HTTP (DASH) refers to one type of these protocols which has been standardized in the 3GPP [4]. Each video file is encoded at multiple bit rates within the server, and thus enables channel aware quality selection. This selection is currently user-driven, yet it increases the risk of buffer underrun and video stops when users greedily request high bitrates that require more resources than the amount calculated by the resource allocator. Hence, a shift towards selection becoming network-centric is gaining momentum in current research to bridge the gap between the decisions of resource allocator and the user device especially in multi-user scenarios [5]. As such, an optimized end-to-end performance can only be achieved by jointly selecting the video quality and resource sharing among the mobile users. In addition, joint decisions allow the network, during low load scenarios, to pre-buffer large portions of the video or increases the quality, thus strikes a balance between energy-saving and user saisfaction. During high load scenarios, as users experience different channel conditions, the network can fairly select the quality and secure the necessary amount of radio resources for each user.

In essence, DASH schemes aim to improve the Quality of Service (QoS) by minimizing the number and durations of stops, and initial buffer delays while maximizing the video quality measured by the bitrate [3]. Current network-centric DASH decisions are based either on previous or future channel conditions. *Non-predictive* DASH adopts reported measurements from user device to calculate the amount of resources and video quality of each user for the next time slot. On the other hand, *Predictive*-DASH (P-DASH) leverages upcoming channel rates to calculate long-term decisions [6], [7]. Compared to the non-predictive scheme, P-DASH promised significant energy savings, user fairness, and resource utilization [6]–[10]. The energy-efficient P-DASH in [6] was able to predict the users with poor channel conditions in the future and pre-buffers their content ahead. Thus, avoids stalls and quality degradation in poor future conditions. Similarly, the P-DASH in [10] provided a higher video quality and less number of video stops compared to traditional *non-predictive* DASH approaches in high load scenarios.

Manuscript received November 28, 2016; revised May 9, 2017 and September 11, 2017; accepted November 14, 2017. Date of publication December 6, 2017; date of current version February 9, 2018. The associate editor coordinating the review of this paper and approving it for publication was L. Musavian. *(Corresponding author: Ramy Atawia.)*

R. Atawia is with the Department of Electrical and Computer Engineering, Queen's University, Kingston, ON K7L 3N6, Canada (e-mail: ramy.atawia@queensu.ca).

H. S. Hassanein is with the School of Computing, Queen's University, Kingston, ON K7L 3N6, Canada (e-mail: hossam@cs.queensu.ca).

A. Noureldin is with the Department of Electrical and Computer Engineering, Royal Military College of Canada, Kingston, ON K7K 7B4, Canada (e-mail: aboelmagd.noureldin@rmc.ca).

Color versions of one or more of the figures in this paper are available online at http://ieeexplore.ieee.org.

Digital Object Identifier 10.1109/TWC.2017.2777988

While both DASH approaches rely on reported or predicted information, developing *robust* techniques became of paramount importance. In essence, a robust technique defines a certain level of constraint satisfaction that has to be met by the decision maker while solving a problem accommodating uncertain or erroneous information. In case of DASH, reported channel measurements are typically subjected to delays and errors due to the random behaviour of wireless channel [11], [12]. Our recent work on predictive streaming with fixed quality (i.e. non-DASH) [13]–[15] studied the challenges in assuming *ideal* predictions and demonstrated the importance of adopting *robust* QoS constraints to define a probabilistic satisfaction level which limits the service degradations when actual rates fall below their predicted values. The impact of such uncertainties, on the QoS and resource utilization, will be more significant in the case of *P-DASH* where both the future resources and qualities are jointly determined by the network.

This paper introduces a *predictive* DASH framework that is *robust* to rate uncertainties, and thus guarantees both QoS satisfaction and video quality fairness among the users over the time horizon. The contributions of this paper are summarized as follows:

1) We propose a network-centric *Robust Predictive*-DASH (RP-DASH) approach that seeks joint optimization of radio resource sharing and video quality selection for each user during an anticipated time horizon using future predicted rates and mobility traces. The main objective is to achieve *long-term* quality fairness among the users over the time horizon while avoiding the video stops due to buffer underrun in order to maximize the QoS. Unlike non-predictive counterparts, the proposed approach allows the network to pre-buffer future video content in high quality to users with poor anticipated rates. Such users will be able to stream the pre-buffered high quality content during poor radio conditions resulting in higher fairness.
2) We introduce a *stochastic* optimization model based on Chance Constrained Programming (CCP) to cap the risk of QoS violation, under rate uncertainties, by a certain predefined level. Such *probabilistic* level allows the operator to control the trade-off between predication gains (i.e. long-term quality fairness) and the QoS violation (i.e. video stops) during uncertain situations. In principle, CCP incorporates the future rates as random variables to capture the uncertainties resulting from imperfect prediction and channel variations. This model differs from existing predictive DASH approaches which adopt deterministic constraints with average values of predicted rates. Hence, such approaches will not be robust when users experience lower rate values than the average value adopted in allocation of resources.
3) In order to solve the proposed stochastic model, a closed form solution that replaces the probabilistic information must be derived. To that end, we use Scenario Approximation (SA) to obtain a deterministic model based on both: the discrete Probability Density Function (PDF) of random modelled rates, and the predefined probabilistic level. While the decision is taken over a time horizon and for both resources and quality, conventional SA results in a combinatorial complexity. As such, we introduce a linear approximation to aggregate the dependency between the time horizon constraints which reduces the formulation to a polynomial model. Such approximation is said to be *safe* since the resulting solution satisfies the predefined QoS level in the *probabilistic* CCP model.
4) While SA provides benchmark solutions for the robust approach, mobile operators strive to minimize the effort of obtaining the discrete PDF. Hence, we propose a second deterministic model based on Gaussian Approximation (GA) that only requires the variance and the inverse Cumulative Density Function (CDF) of predicted rate which is assumed to be normally distributed. Although GA resulted in unsafe allocation (i.e. violated the QoS level) in our prior energy-efficient predictive work [15], recent error models [12] report the validity of Gaussian distribution in representing the rate uncertainty. As such, applying GA in the proposed P-DASH delivery and comparing its performance to SA will unveil the trade-off between robustness and error modelling cost on one hand, and prediction gains on the other hand
5) We propose a low-complexity guided heuristic search algorithm to obtain real-time solutions for the deterministic equivalent GA formulation. Although the formulated model can be optimized by commercial solvers, real-time solutions are not attainable by conventional numerical techniques. Our guided heuristic exploits the problem's distinct features to devise an initial feasible solution. This solution is iteratively optimized using the basis of predictive and robust optimization. Simulation results demonstrate the competence of such guided heuristic to satisfy the QoS level without significant degradation of the selected video quality when compared to optimal solutions (obtained from commercial solvers).

The paper is organized as follows. In Section II we provide a background on DASH and robust stochastic-based optimization. Section III presents the preliminaries, system model, and the robust probabilistic formulation. Section IV and Section V introduce the *Scenario* and *Gaussian* based deterministic formulations and their linearized conservative forms. The low complexity guided heuristic is presented in Section VI, simulation results are discussed in Section VII and finally, we conclude the paper in Section VIII.

II. Background and Related Work

A. Dynamic Adaptive Streaming Over HTTP (DASH)

DASH was essentially introduced to improve the user experience and resource utilization under wireless channel fluctuations [2]. The video file is split and delivered in the form of small segments where the quality of each segment is adapted proportionally to the user's channel condition. In particular, low-quality segments are selected when the user is experiencing low channel rates (e.g. user at the cell edge)

in order to avoid video stalling. On the contrary, high-quality segments are delivered when peak channel rates are observed (e.g. user at the cell center) to exploit the available radio resources and improve the user's experience. The original DASH protocol relies on the user device, aware of the video-specific information and channel conditions, to select the segment quality and request it from the streaming server. Such user-centric approach, however, is unaware of the total network load and other users demands which are considered by the resource allocator. Therefore, a user might select a high-quality level, due to the high measured channel rate, although the network resource allocator will not necessarily devote the whole radio resources to that user in the next time slot. Such limited resources, selected by resource allocator, might not be sufficient to deliver the high-quality segment, requested by the user, and thus increases the risk of video stalling [5].

Research efforts are currently concerned with shifting the DASH from a user-centric decision to a network driven decision in order to bridge the gap between the objectives of individual users and the resource allocator [16]. To that end, the network jointly optimizes the segments qualities and the resource sharing among the users. Thus, avoids the greedy quality selection by the users when they overestimate the available radio resources. At the Base Station (BS), the resource allocator overwrites the user's requested quality before forwarding it to the server [16]. Recent BS storage capability provides another implementation flexibility where the video is locally cached with different quality representations, and the segments are sent at the resource allocator's quality.

Conventional network-centric DASH [17]–[19] adopts recent channel measurements, reported by the user's device, to optimize the network gains (e.g. resource utilization) and QoS (e.g. quality and interruptions). Each user reports the current channel conditions to the network which in turn calculates both the segment's quality and the amount of resource share for each user at a certain time slot. These reactive decisions only achieve local optimal network performance without QoS guarantees due to overlooking the users' future radio conditions. *Predictive*-DASH (P-DASH) [6]–[10], oppositely, foresee the upcoming radio conditions to derive long-term policy while allocating the current resources. For example, two users at the cell center (i.e. good radio conditions), one is moving towards the cell edge while the other will not move. As the former experiences poor radio conditions in the future, the resource allocator must prioritize this user by allocating more resources during peak radio conditions. Long-term fairness in terms of quality and stalls can be achieved by either pre-buffering the future content or increasing the current video quality. On the contrary, users in poor conditions and moving towards high channel rates will be allocated a small amount of resources. An unprecedented challenge is the uncertainty in future information such as user's location and channel rates which makes the *P-DASH* decisions suboptimal or non-robust.

B. Robust Stochastic Optimization

Mobile operators substantially rely on users device measurements to predict the future channel conditions [10], [20]. Therefore prediction accuracy depends on the capabilities of mobile devices and their estimation methods. Nevertheless, the random nature of the received signal level over the wireless channel will cause temporal and spatial variations in the reported measurements and their consequent estimations. Accordingly, relying solely on the average values to represent future channel rates as in [6], [9], and [10] will not guarantee QoS satisfaction. As the predicted rates fall below their average values, the minimal amount of resources allocated to the users in poor radio conditions will not be sufficient to satisfy the selected quality. Similarly, when the channel experiences outages during anticipated peak conditions, the large amount of resources will not be optimally utilized. This is in addition to the increased risk of video stops when high-quality levels are selected for these peaks.

Robust techniques have been discussed in the literature for non-predictive allocations (i.e. without time horizon) in order to handle uncertainties or delays in the instantaneous user reported measurements [21]–[23]. *Stochastic* optimization is typically used to provide a robust formulation of the allocation problem in which the predicted uncertain values are represented as random variables [24]. For the problem at hand, we focus on CCP in which the constraints accommodating random variables are represented in a probabilistic form with a maximum violation degree denoted as $\epsilon \in [0, 1]$. A deterministic equivalent form is then derived to obtain a closed form representation which can be further solved by mathematical optimization techniques.

Robust stochastic work utilizes different techniques such as Scenario Approximation (SA), Gaussian Approximation (GA), Bernstein Approximation (BA) and Markov inequality [12], [14], [22], among others, to obtain the CCP deterministic form. The GA assumes that all the random variables, in the formulation, follow a normal distribution. Their summation results in a multivariate random variable whose mean and covariance is a function of the statistical parameters of each single random variable. This derives a Second order Cone Programming (SoCP) formulation which also incorporates the inverse of the Gaussian Cumulative Density Function (CDF) and the QoS degradation level ϵ. Similarly, the BA adopts the Moment Generating Function (MGF) to develop a SoCP deterministic form that only depends on the support of random variables and the QoS degradation level ϵ as well. The *Markov* inequality [23] on the other hand provides a linear empirical approximation. However, the optimal coefficients for such approximation are not easily attainable and do not model the trade-off between optimality and degree of constraint satisfaction. The SA utilizes the discrete PDF of the random variables to create a scenario tree using all the combinations. The allocator has to ensure that the calculated resources satisfy the scenarios with total probability more than $1 - \epsilon$.

Our earlier work in [13]–[15] focused on robust energy-efficient predictive allocation approaches where the objective was to minimize the energy consumption at a constant video quality. The conventional GA resulted in an unsafe approximation in which the QoS violations surpassed the maximum predefined probabilistic level in the CCP model [15]. This necessitates a new design of CCP in which the per slot

probabilistic level is jointly optimized over the time horizon constraints to consider their interdependence. The BA, on the other hand, resulted in conservative solutions that decreased the energy savings of the predictive scheme [14]. The comparison between GA and BA revealed a trade-off between the predication gains (i.e. energy savings in that case), QoS violations, error modelling cost and computational complexity. The optimization problem in previous work was mainly concerned with striking a balance between the energy consumption (which is a network metric) and the users QoS satisfaction. The SA was not used in previous as it compromises the continuity of the energy-saving problem. This is unlike the problem at hand which balances two QoS metrics, mainly quality fairness and video stops, and solves for both integer and continuous decision variables.

Our proposed *Robust Predictive*-DASH (RP-DASH) scheme aims to optimize the resource sharing and quality of segments over a time horizon such that *long-term quality fairness* is achieved among users while the probability of video stops is kept below the violation degree ϵ. Both SA and GA are adopted to obtain deterministic equivalent forms. This is followed by linear and convex approximations to obtain optimal benchmark solutions by commercial solvers, and a low complexity guided heuristic for real-time allocations.

III. Robust Predictive DASH Formulation

A. Preliminaries

We use the following notational conventions throughout the paper. $\mathcal{X}$ denotes a set and its cardinality is denoted by $|\mathcal{X}|$. Matrices are denoted with subscripts, e.g. $\mathbf{x} = (x_{a,b} : a \in \mathbb{Z}_+, b \in \mathbb{Z}_+)$. $Pr\{x\}$ is the probability of event x. $\mathbb{1}_x$ is an indicator function that is equal to one if event x is true and equals 0 otherwise. $\tilde{r}$ represents a random variable whose expectation is $\mathbb{E}[\tilde{r}]$, its CDF is dented by $\Phi_{\tilde{r}}(x) = Pr\{\tilde{r} \leq x\} = \int_{-\infty}^{x} N(\tilde{r}, t)dt$ and the PDF is $N(\tilde{r})$. The number of realizations in a discrete PDF is denoted by $|J|$ and $r^{(j)}$ denotes the j^{th} realization of random variable $\tilde{r}$. $\Phi(x)$ represents the CDF of a normally distributed random variable with zero mean and unit variance, while its inverse CDF is denoted by Φ_x^{-1} corresponding to the x^{th} percentile.

B. System Model

The system considers a group of BSs, each serves an active user set denoted by $\mathcal{M}$, where the user index is $i \in \mathcal{M}$. The video is transmitted from the server to the Evolved Packet Core (EPC) and then cached at the BS.

1) BS Radio Resources: The active users share the BS resources (airtime fractions) at each time slot t. The resource allocation matrix $\mathbf{x} = (x_{i,t} \in [0, 1] : i \in \mathcal{M}, t \in \mathcal{T})$ represents the fraction of resources devoted to deliver user i content during time slot t.

2) Rate and Mobility Prediction: For the resource allocation, prediction of rate is done by mapping the user's current location to the Radio Environment Map (REM) at the network. The REM contains both the user's locations and the corresponding average rate values denoted as $\bar{r}_{i,t} = \mathbb{E}[\tilde{r}_{i,t}]$. We assume that user's mobility trace is known for the next T timeslots, where each slot is denoted by $t \in \mathcal{T} = \{1, 2, \cdots, T\}$. The mobility can be predicted based on usersâĽ™ predefined paths (e.g. train or bus routes) and supported with today's mobile devices that are typically equipped with localization systems such as Global Positioning System (GPS) and Wi-Fi. Such predictability is supported by measurements in public transportation [11] and verified in existing predictive video delivery [9], [25] which constructed offline REM for a certain geographical area. In real-time, the network adopts GPS-based locations and velocities to estimate users mobility traces and retrieve the corresponding average channel rates from the REM.

3) Predicted Rate Error Model: In order to model prediction uncertainties, future rate is modelled as random variable denoted by $\tilde{r}_{i,t}$. The random variable is either described by 1) its discrete PDF when the realizations and their probabilities are known or 2) the Gaussian distribution in which the standard deviation is denoted by $\sigma_{i,t}$ and can calculated by [14]. Both error rates are depicted in Fig.1(a)-Fig.1(b). This Gaussian distribution error model is motivated by the findings in [13], [20], and [22] and will be used to quantify the trade-off between error PDF modelling and robustness. In both cases, the per slot rate errors are assumed to be independent. Particularly, the error of predicting the rate is function of erroneous rate in REM, variations in the wireless signal (which changes the SINR) and user location uncertainty. These parameters are calculated at each slot based on the independent channel gains [22], [26].

4) Video Quality Selection: Each video segment can be transmitted and played back at quality level $q \in Q$, where Q is the set of possible segment qualities. The binary decision variable $\kappa_{i,t}^{(q)}$ is equal to 1 if the video segment transmitted to user i at time slot t is encoded in quality q, and 0 otherwise. Each segment consists of v_q bytes of data, which depends on the selected quality level q.

5) Per Slot Demand Probabilistic Constraint: In order to experience smooth video steaming, with minimal stalls, the total duration of delivered content should be more than or equal to the elapsed playback time till slot t. Thus, the cumulative allocated data to user i at each time slot t should be more than the total data size of the requested video segments. This is modelled by a probabilistic chance constraint which ensures that the probability of video stops at slot t does not exceed $\epsilon_{i,t}$. The playback duration of each segment is denoted by $\tau_{i,t}$.

The RP-DASH scheme in this paper aims to calculate both the airtime fractions $x_{i,t}$ and segments quality $\kappa_{i,t}^{(q)}$ for each user i at time slot t such that all users experience fair video qualities while meeting the QoS level. Particularly, QoS is said to be satisfied when users experience video stops, due to buffer underrun, with probability below ϵ.

C. Stochastic Chance Constrained Formulation

The introduced robust P-DASH and fair quality selection is formulated based on Chance Constrained Programming (CCP)

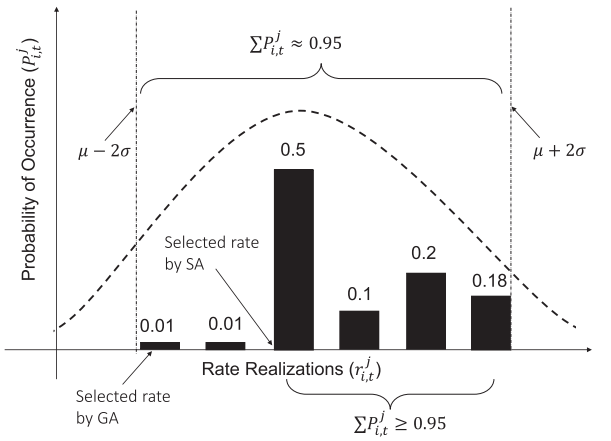

(a) Example of GA more conservative than SA

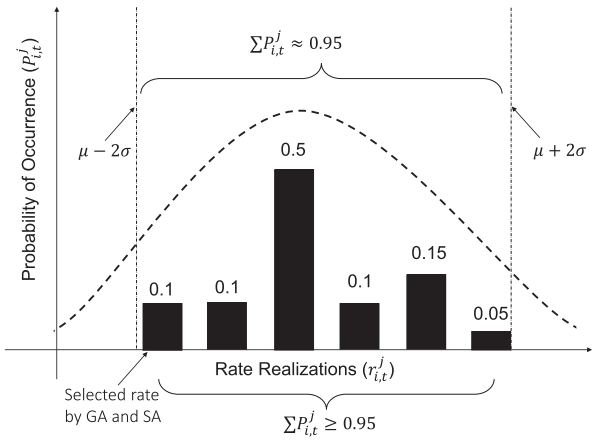

(b) Example of GA equal conservative to SA

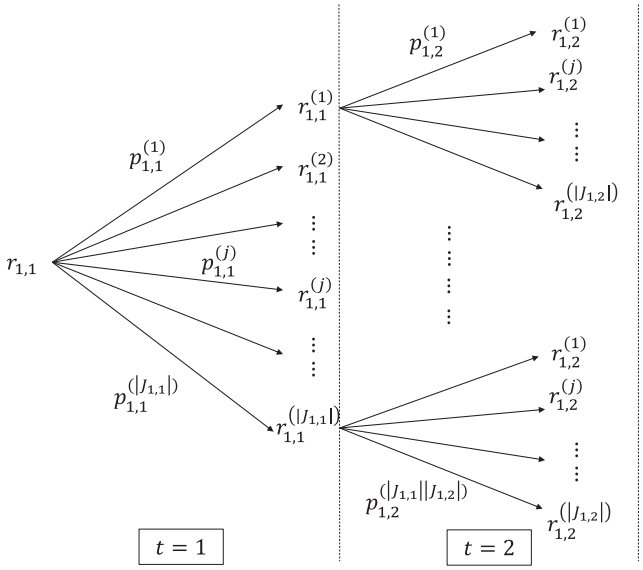

(c) Conventional SA

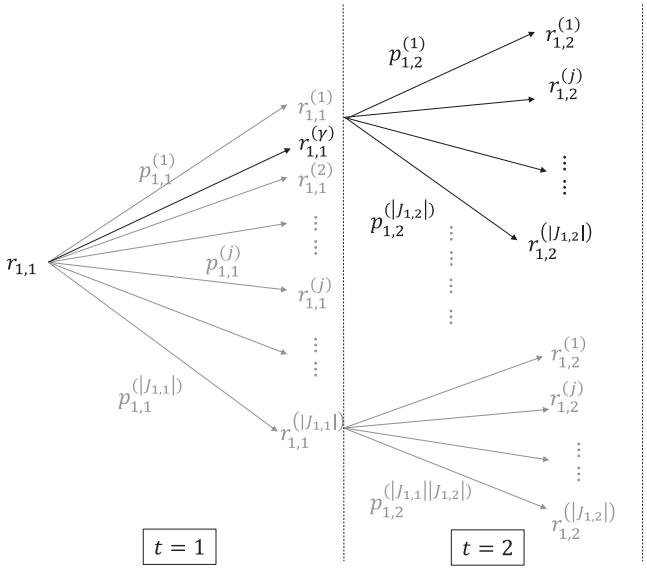

(d) Linear lookback SA

Fig. 1. Illustration of SA and GA operations.

as follows:

$$\begin{aligned}
&\underset{\mathbf{x},\kappa}{\text{maximize}} \quad \left\{ \min_{\forall i \in \mathcal{M}} \sum_{\forall t \in \mathcal{T}} \sum_{\forall q \in Q_i} \kappa_{i,t}^{(q)} \upsilon_q \right\} \\
&\text{subject to: C1:} \quad Pr\left\{ \sum_{t'=0}^{t} \tilde{r}_{i,t'} x_{i,t'} \geq \sum_{t'=0}^{t} \sum_{\forall q \in Q_i} \kappa_{i,t'}^{(q)} \upsilon_q \right\} \\
&\qquad \geq 1 - \epsilon_{i,t}, \quad \forall i \in \mathcal{M}, \ \forall t \in \mathcal{T}, \\
&\text{C2:} \quad \sum_{t'=0}^{t} \sum_{\forall q \in Q_i} \kappa_{i,t'}^{(q)} \tau_{i,t'} \geq t, \quad \forall i \in \mathcal{M}, \ \forall t \in \mathcal{T}, \\
&\text{C3:} \quad \sum_{q \in Q_i} \kappa_{i,t}^{(q)} \leq 1, \quad \forall i \in \mathcal{M}, t \in \mathcal{T}, \\
&\text{C4:} \quad \kappa_{i,t}^{(q)} \in \{0,1\}, \quad \forall i \in \mathcal{M}, t \in \mathcal{T}, \\
&\text{C5:} \quad \sum_{i=1}^{|\mathcal{M}|} x_{i,t} \leq 1, \quad \forall t \in \mathcal{T}, \\
&\text{C6:} \quad x_{i,t} \geq 0, \quad \forall i \in \mathcal{M}, \ t \in \mathcal{T}. \qquad (1)
\end{aligned}$$

$\epsilon_{i,t} \in [0,1]$ is the probability that the QoS of user i is unsatisfied at time slot t, where $\epsilon_{i,t} = 1$ is the maximum QoS violation. The objective function aims to maximize the minimum total quality of each user to attain the fairness among the users over the time horizon. The QoS chance constraint in C1 guarantees that the total delivered content to the user satisfies the anticipated demand (function of the selected quality) by a minimum probability of $1 - \epsilon$ while considering uncertainties in future rates. The constraint in C2 complements C1 to ensure that the total duration of the selected segments should be greater than the elapsed playback time to avoid video stops. C3 and C4 ensure that, for each user, only one quality level is selected at a given time slot. The fifth constraint C5 models the limited resources at each base station by ensuring that the sum of the airtime fractions is less than 1 second which is the duration of the allocation slot. The last constraint C6 ensures the non-negativity of the decision variable. Indeed the above formulation does not have a closed form solution due to the probabilistic constraint C1. As such, we will initially adopt the SA to obtain a deterministic equivalent form in the next section.

IV. Scenario Based Approximation

A. Multi-Stage Scenario Based Approximation

The Scenario approximation adopts the discrete Probability Density Function (PDF) of the uncertain rates to derive a deterministic representation for the probabilistic constraint. The PDF of every rate $\tilde{r}_{i,t}$ contains all the realizations $r_{i,t}^{(j)}$ and their probabilities $p_{i,t}^{(j)}$ to construct the scenarios over the time horizon. The approximation ensures that resource allocations and quality selections satisfy the scenarios whose total probability of occurrence is more than the defined QoS level (i.e. $1-\epsilon$). Each scenario corresponds to one combination of the possible realizations of the uncertain rates in C1. For example, the constraint in the second time slot includes the rates in both the first and second time slot. The scenarios will comprise all the possible combinations of the realizations of these two rates. As illustrated in Fig. 1(c), the first scenario consists of $r_{1,1}^{(1)}$ and $r_{1,2}^{(1)}$. Where $r_{1,1}^{(1)}$ represents the first realization of the rate at t=1, and $r_{1,2}^{(1)}$ is the first realization of the rate at t=2, both for the first user. The probability of this scenario will be the product of the individual probabilities (i.e. $s_{1,2}^{(1)} = p_{1,1}^{(1)} \times p_{1,2}^{(1)}$). The deterministic equivalent of C1 in Eq. 1 is captured by C7-C9 below

$$\underset{\mathbf{x},\kappa,\delta}{\text{maximize}} \left\{ \min_{\forall i \in \mathcal{M}} \sum_{\forall t \in \mathcal{T}} \sum_{\forall q \in Q_i} \kappa_{i,t}^{(q)} v_q \right\}$$

$$\text{subject to: C7:} \sum_{t'=0}^{t} r_{i,t'}^{(j)} x_{i,t'} \geq \delta_{i,t}^{(j)} \sum_{t'=0}^{t} \sum_{\forall q \in Q_i} \kappa_{i,t'}^{(q)} v_q,$$

$$\forall i \in \mathcal{M}, \quad \forall t \in \mathcal{T}, \ \forall j \in \mathcal{J}_{i,t},$$

$$\text{C8:} \quad \sum_{j \in \mathcal{J}_{i,t}} s_{i,t}^{(j)} \delta_{i,t}^{(j)} \geq 1 - \epsilon_{i,t}, \quad \forall i \in \mathcal{M}, \ t \in \mathcal{T},$$

$$\text{C9:} \quad \delta_{i,t}^{(j)} \in \{0, 1\}, \quad \forall i \in \mathcal{M}, \ t \in \mathcal{T}, \ j \in \mathcal{J}_{i,t},$$

$$\text{(C2 - C6)} \tag{2}$$

where $r_{i,t}^{(j)}$ is the j^{th} realization of the uncertain predicted rate at time slot t for user i. $s_{i,t}^{(j)}$ is the probability of the j^{th} scenario at time slot t for user i. $\delta_{i,t}^{(j)}$ is a binary decision variable which equals to 1 if the j^{th} scenario at slot t must be satisfied by the decision variable and equals 0 otherwise (C9). Constraint C8 guarantees that the total probability of all the satisfied scenarios exceeds the minimal QoS level $1-\epsilon$.

While the above formulation is deterministic and robust, it poses the following three main challenges to the solver:

1. Non-linearity: due to the joint optimization of quality and airtime fractions, the right hand side in C7 will be non-linear (both decision variables are multiplied). Despite the dimensions of C7, the problem is NP-hard and reaching the optimal solution is not guaranteed.
2. Exponential complexity: the QoS constraint at each time slot is a function of the rate in both the current and preceding slots (C7 in Eq. 2 and Fig. 1). Thus, at each time slot t the number of considered scenarios will be $\prod_{t'=0}^{t} |J_{i,t'}|$, where $|J_{i,t'}|$ is the number of realizations of the uncertain rate $r_{i,t'}$. Assuming that all the rates have equal number of realizations (i.e. $|J_{i,t'}| = |J_i|$), thus the total number of scenarios for each time slot constraint per user will be $(|J_i|)^{(t)}$.
3. Explicit rate information: the scenario-based approximation requires the exact values of realizations for all the rates and their corresponding probabilities. This requires collecting large number of samples for each achievable channel rate value in order to construct an accurate discrete PDF. Due to the large number of physical layer configurations such as Multiple Input Multiple Output (MIMO) and Modulation and Coding Scheme (MCS), more possible rates can be achieved. Hence, increases the burdens of prediction stage.

In the next subsection we address the first two challenges while the third challenge is tackled separately in the next section by the Gaussian based approximation. We note that the first challenge can be tackled by simple linearization since one of the decision variables is binary, but the other challenges require more effort.

B. Linear Look-Back Scenario Approximation

The nonlinearity of QoS constraint C7 is solved by exploiting the problem's structure. The scenario decision variable $\delta_{i,t}^{(j)}$ is governed by the QoS constraint C8, as such a minimal number of scenarios should be satisfied (i.e. $\delta_{i,t}^{(j)} = 1$). For each satisfied scenario (i.e. $\delta_{i,t}^{(j)} = 1$), the corresponding airtime allocation (i.e. left hand side of C7) should guarantee the satisfaction of the selected demand (i.e. video quality) while considering the worst case of the selected scenario. The objective function plays the main role in discarding the scenarios (i.e. $\delta_{i,t}^{(j)} = 0$) whose realizations have very low values. In that case, both sides of C7 are equal to zero, and the scenario is not satisfied by the calculated airtime fractions.

A new linear representation for C7 in Eq. 2 is introduced to capture the above strategy and avoid the exponential complexity due to considering the realizations of all previous time slots. Instead, the new formulation considers a linear look-back on the preceding rate realizations to decrease the large number of scenarios at each time slot. Only one conservative realization denoted by $r_{i,t}^{(\gamma)}$ is selected to represent each of the rates in the previous slots. The number of scenarios at slot t will depend only on the realizations in this slot ($|J_{i,t}|$) and the number of previous slots ($t-1$) instead of all the realizations of the latter. In order words, $|J_{i,t}| \times (t-1)$ scenarios are considered instead of $(|J_i|)^{(t)}$. The new linear formulation is represented as follows:

$$\underset{\mathbf{x},\kappa,\delta,\mathbf{Y}}{\text{maximize}} \sum_{i=1}^{|\mathcal{M}|} Y_i$$

$$\text{subject to: C10:} \sum_{t'=0}^{t} \sum_{\forall q \in Q_i} \kappa_{i,t'}^{(q)} v_q - \left(\sum_{t'=0}^{t-1} r_{i,t'}^{(\gamma)} x_{i,t'} + r_{i,t}^{(j)} x_{i,t}\right)$$

$$\leq \mathbb{B}(1 - \delta_{i,t}^{(j)}), \quad \forall i \in \mathcal{M}, \ t \in \mathcal{T},$$

$$\text{C11:} \quad \sum_{j \in \mathcal{J}_{i,t}} p_{i,t}^{(j)} \delta_{i,t}^{(j)} \geq 1 - \epsilon_{i,t}, \quad \forall i \in \mathcal{M}, \ t \in \mathcal{T},$$

$$\text{C12:} \quad \sum_{t'=0}^{t} \sum_{\forall q \in Q_i} \kappa_{i,t}^{(q)} v_q \geq Y_i, \quad \forall i \in M,$$

$$\text{(C2 - C6, C9)} \tag{3}$$

The minimum function operator in the objective of Eq. 2 was replaced by introducing auxiliary variable Y_i and the fairness constraint C12 which must be satisfied for all users. C10 represents the linear look-back constraint in which $p_{i,t}^{(j)}$ is the probability of realization j of channel rate $r_{i,t}$ and $\mathbb{B}$ is a very large number that forces the airtime allocation to satisfy the demand when scenario j is considered. $r_{i,t}^{(\gamma)}$ approximates the channel rates of the preceding timeslots and can be calculated as follows

$$\begin{aligned} &\underset{\theta, r_{i,t}^{(\gamma)}}{\text{minimize}} \ r_{i,t}^{(\gamma)} \\ &\text{subject to: } r_{i,t}^{(\gamma)} \geq \sum_{j \in \mathcal{J}_{i,t}} r_{i,t}^{(j)} \theta_j \\ &\qquad \theta_j \sum_{j'=1}^{j} p_{i,t}^{(j')} \geq \epsilon, \quad \forall j \in \mathcal{J}_{i,t} \\ &\qquad \theta_j \in \{0, 1\} \end{aligned} \tag{4}$$

The objective function in Eq. 4 aims to select the optimal value of the aggregated rate $r_{i,t}^{\gamma}$ for the slot realizations such that very low values with conservative solutions and high values with non-robust solutions are ignored. The first constraint ensures that the calculated value of $r_{i,t}^{\gamma}$ surpasses some realizations due to their low values; where ignoring such realizations avoid conservative solutions. The second constraint guarantees that the sum of probability of the ignored realizations is below the degradation level ϵ, to achieve robustness. The last constraint defines θ as a binary decision variable. Since the objective function is minimization which is subjected to the second constraint, the decision variable is $\sum_j \theta_j = 1$. Thus only one realization value is selected to satisfy the first constraint.

V. Gaussian Based Approximation

A. Gaussian Linear Conservative Formulation

The third challenge of Scenario Approximation (SA) is tackled by adopting the Gaussian Approximation (GA) which does not require the explicit realizations and their probabilities for all future rates. Instead, GA obtains a deterministic closed form for C1 using the CDF of multivariate random variables. Thus the probabilistic constraint C1 is replaced by the following deterministic form

$$\begin{aligned} &Pr\left\{ \sum_{t'=0}^{t} \tilde{r}_{i,t'} x_{i,t'} \geq \sum_{t'=0}^{t} \sum_{\forall q \in Q_i} \kappa_{i,t'}^{(q)} v_q \right\} \\ &= 1 - \int_{-\infty}^{D_{i,t}} N(\mathbf{r}, \mu, \Sigma) d\mathbf{r} \\ &= 1 - \frac{\Phi(\frac{D_{i,t} - \mu_{i,t}}{\Sigma_{i,t}}) - \Phi(\frac{-\mu_{i,t}}{\Sigma_{i,t}})}{S_{i,t}} \geq 1 - \epsilon_{i,t}, \end{aligned} \tag{5}$$

Using the inverse CDF, the following closed form can be obtained:

$$\mu_{i,t} + S_{i,t} \Phi_{\epsilon_{i,t}}^{-1} \Sigma_{i,t} \geq D_{i,t}, \quad \forall i \in \mathcal{M}, \ t \in \mathcal{T}, \tag{6}$$

where:

$$\begin{aligned} S_{i,t} &= \prod_{t'=0}^{t} \left(\Phi(\frac{r_{i,t'}^{(u)} - \bar{r}_{i,t'}}{\sigma_{i,t'}}) - \Phi(\frac{r_{i,t'}^{(l)} - \bar{r}_{i,t'}}{\sigma_{i,t'}}) \right) \\ \mu_{i,t} &= \sum_{t'=0}^{t} \bar{r}_{i,t'} x_{i,t'}, \\ \Sigma_{i,t} &= \sqrt{\sum_{t'=0}^{t} x_{i,t'}^2 \sigma_{i,t'}^2}, \\ \sigma_{i,t'}^2 &= E[(\tilde{r}_{i,t'} - \bar{r}_{i,t'})^2], \\ D_{i,t} &= \sum_{t'=0}^{t} \sum_{\forall q \in Q_i} \kappa_{i,t'}^{(q)} v_q \end{aligned}$$

$r_{i,t}^{(l)}$ and $r_{i,t}^{(u)}$ are the lower and upper bounds of the realizations of future predicted rate $\tilde{r}_{i,t}$ (i.e. the support). Typical values of the channel rates in the current and future networks are more than the corresponding variance values (i.e. $\mu_{i,t} >> \Sigma_{i,t}$) and thus $\Phi(\frac{-\mu_{i,t}}{\Sigma_{i,t}}) \approx 0$. $S_{i,t}$ is used to normalize the truncated probability distribution of the random rates.

The above deterministic form, however, is a mixed integer quadratic constrained programming which is NP-hard. A linear approximation is adopted, which turns the problem to NP-complete. This is done by the budgeted robust approximation of [21] on Eq. 6 as follows. Let $\Sigma_{i,t}^{(L)} = \sum_{t'=0}^{t} |x_{i,t'} \sigma_{i,t'}|$, thus $\Sigma_{i,t} < \Sigma_{i,t}^{(L)}$, and $\Phi(\frac{1}{\Sigma_{i,t}}) > \Phi(\frac{1}{\Sigma_{i,t}^{(L)}})$. This guarantees the satisfaction of C1 by substituting $\Sigma_{i,t}$ with $\Sigma_{i,t}^{(L)}$. Such approximation will result in a linear but conservative formulation compared to the original Gaussian approximation.

The final deterministic mixed integer linear equivalent for the RP-DASH in Eq. 1 is summarized as

$$\begin{aligned} &\underset{\mathbf{x}, \kappa, \mathbf{Y}}{\text{maximize}} \ \sum_{i=1}^{|\mathcal{M}|} Y_i \\ &\text{subject to: C13:} \quad \mu_{i,t} + S_{i,t} \Phi_{\epsilon_{i,t}}^{-1} \Sigma_{i,t}^{L} \geq D_{i,t}, \\ &\qquad \forall i \in \mathcal{M}, \quad t \in \mathcal{T}, \\ &\qquad \text{(C2 - C6)} \end{aligned} \tag{7}$$

B. Discussion and Comparison to Scenario Approximation

We are now interested in discussing both the robustness and conservatism of the GA and compare them to those of the SA. In Fig. 1(a)-Fig. 1(b), both the GA and SA are illustrated for one time slot where ϵ is set to 0.05. For the Gaussian distribution, 0.95 of the samples lies within the interval $[\mu - 2\sigma, \mu + 2\sigma]$. As such, the GA based RP-DASH will be adopting the lowest rate realization as depicted in Fig. 1(a). On the other hand, the SA will only select the highest rates whose total probabilities will sum up to 0.95. This results in a higher rate value selected by

the SA and thus less conservative solution. When the majority of total probabilities are above the mean value, GA is more conservative, while roughly symmetric PDF around the mean will result in selecting the same rate realization as SA (i.e. equal conservative). In conclusion, the GA will always select the same or lower rate compared to the SA which makes the former a more conservative and robust approximation at each time slot specially when rate distribution is shifted above the predicted mean value.

Both the original multi-stage SA and the linear look-back SA are illustrated in Fig. 1(c)-Fig. 1(d) for two consecutive time slots. The later will be more conservative since it ignores the rate realizations above $r^{(\gamma)}$ in the first time slot. These values could have been combined with the rate realizations in the next time slot and resulted in less conservative solution.

VI. Real-Time Optimizer

This section introduces the guided heuristic algorithm to obtain real-time solutions for the formulated RP-DASH problem. This is in addition to analyzing its computational complexity.

A. Limitations of Optimal Commercial Solvers

The Scenario-and Gaussian-based robust formulations in Eq. 3 and Eq. 7 are represented in mixed integer linear programming forms. The main advantage of these forms is that an optimal feasible solution can be obtained using branch and bound or simplex techniques. Such conventional techniques are currently well developed and implemented in many commercial solvers such as Gurobi [27]. These solvers use their own developed heuristic algorithms to calculate an initial feasible solution which satisfies the constraints. Other neighbouring solutions are then explored by means of branch and bound or simplex algorithms, while using the duality gap to evaluate the optimality of each solution. Although zero or low duality gaps (i.e. optimal solutions) can be achieved by commercial solvers, the execution time highly increases with the problem's dimensions (i.e. number of constraints and decision variables). A guided heuristic algorithm is proposed in this paper to provide a real-time feasible solution with low optimality gap from commercial solvers solutions.

B. Guided Real-Time Heuristic

The introduced guided heuristic search algorithm is aware of the problem's structure that includes the interdependency between the constraints and their impact on the value of objective function. This is in addition to considering the motive of robust and predictive allocation in calculating the airtime fractions and video qualities. In essence, the algorithm starts by satisfying all the QoS constraints using the available radio resources while ignoring the objective function in that stage. This first stage contains two problem specific knowledge: 1) the buffering capabilities of the users and 2) the direct relation between the QoS and the resource limitation constraints. The former knowledge can be used to push the video content in advance and thus avoid stalling in congested time slots. In the next step, the value of objective function is maximized while exploiting three other problem features: 1) the trade-off between the fairness (i.e. the objective function) and the above-mentioned two constraints, 2) the time horizon and the buffer status of each user, and 3) the competition between the users, experiencing different channels rates, on the radio resources of one time slot.

Algorithm 1 Initialization and QoS Satisfaction Stages of Guided Heuristic

Input : Users: $\mathcal{M}$, Time Horizon: $\mathcal{T}$, Average Predicted Rates: $\bar{R}$, Rate Variances: Σ, Maximum Violation: ϵ and Video Qualities: Q;
Output : X;
Initialization: $X = \emptyset$, $\kappa = \emptyset$ $N_t = 0$ $\forall t \in T$
1 **Define:** $\mathcal{R}_{i,t} = \bar{r}_{i,t} - S_{i,t}\Phi^{-1}_{\epsilon_{i,t}}\sigma_{i,t}$;
2 **for** $i \in \mathcal{M}$ **do**
3 **for** $t \in \mathcal{T}$ **do**
4 Set $\kappa^0_{i,t} = 1$;
5 Set C13 of Eq. 7 to an equality and solve for $x_{i,t}$;
6 $N_t = N_t + x_{i,t}$;
7 **end**
8 **end**
9 **for** $t \in \mathcal{T}$ **do**
10 **if** $N_t > 1$ **then**
11 Set $k = t - 1$;
12 **while** $k > 0$ **do**
13 Calculate the residual airtime $\Delta x_{i,t} = N_t - 1$;
14 Calculate the demanded airtime $\Delta x_{i,k} = \Delta x_{i,t} \times \frac{\mathcal{R}_{i,t}}{\mathcal{R}_{i,k}}$;
15 $i* = argmax x_{i,k} \forall i \in \mathcal{M}$;
16 **if** $N_k + \Delta x_{i*,k} \leq 1$ **then**
17 Update $x_{i*,k}$, $x_{i*,t}$, N_t and N_k ;
18 break;
19 **end**
20 $k = k - 1$;
21 **end**
22 **end**
23 **if** $N_t > 1$ **then**
24 Return Infeasible Problem;
25 **end**
26 **end**
27 return X

The heuristic implements two main consecutive stages summarized in Algorithm 1 and Algorithm 2, respectively and are detailed as follows:

1) Satisfaction of Minimal Quality: In this initial stage (Algorithm 1), the lowest video quality is assigned to all users over the time horizon (Algorithm 1, line 3). Then, the amount of airtime that satisfies this quality level is calculated (line 4) and used to update the total amount of allocated resources at each time slot (line 5). Such allocation guarantees the satisfaction of QoS constraint C13 in Eq. 7.

However, in high load scenarios, due to high QoS levels (i.e. $1 - \epsilon$) or a large number of users, the total allocated

Algorithm 2 Optimization Stages of Guided Heuristic

Output: X and κ;
1 **Define:** $\mathcal{R}_{i,t} = \bar{r}_{i,t} - S_{i,t}\Phi^{-1}_{\epsilon_{i,t}}\sigma_{i,t}$;
2 **for** $t \in \mathcal{T}$ **do**
3 **while** $N_t < 1$ **do**
4 Calculate $\mathcal{V}_{i,t} = \sum_{t'=0}^{t}\sum_{\forall q \in Q}\kappa^{(q)}_{i,t'}\upsilon_q$ for all users;
5 **for** $i \in \mathcal{M}$ **do**
6 Calculate a possible higher quality level $\kappa^{(q')}_{i,t}\upsilon_{q'}$;
7 Calculate the required airtime $\Delta x_{i,t}$ to satisfy $\kappa^{(q')}_{i,t}\upsilon_{q'}$;
8 Update $\mathcal{V}_{i,t}$ using $\kappa^{(q')}_{i,t}\upsilon_{q'}$;
9 **end**
10 Select the set of users l with minimum $\mathcal{V}_{i,t}$;
11 Select user k from l with minimal $\Delta x_{i,t}$;
12 Update N_t, $x_{k,t}$, and $\kappa^{(q)}_{k,t}$;
13 **if** *l is empty* **then**
14 **while** $t' < T$ **do**
15 Select user i with maximum $(\mathcal{R}_{i,t}) \times (r_{i,t'} - r_{i,t})$;
16 Repeat lines $5-6$ and line 11 for user i with $t = t'$;
17 **end**
18 **end**
19 **end**
20 **end**
21 return X and κ

resources in a certain time slot might violate the airtime constraint C5 in Eq. 1. Accordingly, the preceding time slots with vacant resources will be used to pre-buffer the content of the highly loaded time slots as depicted in lines 11-21 of Algorithm 1. While efficient exploitation of the radio resources is mandatory, the algorithm selects the user with the highest achievable rate in this preceding slot and pre-buffers the content (lines 13-16). Thus, less airtime is consumed and the chance of satisfying the radio resource constraint C5 is increased. In case of non-vacant resources, the problem is said to be infeasible (lines 23-25). Other bounding and streaming constraints are implicitly satisfied by the above iterative procedure.

2) Optimizing Long-Term Fairness: This stage (Algorithm 2) aims to maximize the value of objective function without violating any of the aforementioned satisfied constraints. While the objective is to maximize the long-term quality for each user, the algorithm tries to achieve this on both the current and the future time slots. In each time slot with vacant resources, both the cumulative quality and the required airtime to increase the current slot's quality are calculated for each user (lines 3-7). The user with minimal quality (both cumulative and increased values) is selected as long as the required airtime is less than the available vacant resources (line 9). In case of more than one user with the same quality, the one that requires less airtime is selected (line 10). This procedure is repeated for all users as long as there are vacant resources in the current slot and the video quality is improving.

For low-load scenarios, due to either a small number of users or high achievable rates, the resources at a certain time slot might not be fully utilized. As such, predictive allocation is performed in order to maximize the quality of the users experiencing their highest channel conditions in the current time slot. This is modelled by calculating the ratio between the achievable rate in this time slot and the minimal future rate. Thus, users with peak radio conditions who are heading towards the cell edge (line 14) will have the highest ratio and thus can use these vacant resources to increase the quality of future video content (lines 13-16). The achievable rate used to calculate all the airtime allocations is a function of the average value, variance, CDF and QoS level as derived in C13 of Eq. 7.

C. Algorithm Complexity

The first part of the heuristic (i.e. Algorithm 1) consists of two successive loops, the first is in lines 1-9 and has a complexity $O(MT)$. The second loop, however, has a higher complexity of $O(MT^2)$ due to revisiting the preceding time slots in lines 9-27. Similarly, the second part of the heuristic (i.e. Algorithm 2) has a complexity of $O(QMT^2) \approx O(MT^2)$ due to the relatively small number of available quality levels compared to the length of the time horizon. The complexity of the whole proposed heuristic is $O(MT^2)$ which is lower than numerical optimization methods.

VII. Performance Evaluation

A. Simulation Setup

We simulate the proposed RP-DASH using the Long Term Evolution (LTE) module in Network Simulator 3 (ns-3) [28] which is integrated with Gurobi commercial solver [27] to obtain optimal solutions for all the formulated problems. The fading model of 3GPP defined in [29] is added to the received power at the user device to apply variations in predicted rate. Users follow random predefined paths within the cell coverage region at varying velocities from 25 to 40 km/h, which correspond to typical values in urban areas. All the simulation parameters and values are presented in Table I, and the average of all output results, over 50 simulation runs, is reported in the following subsections. We compare the introduced RP-DASH scheme with an existing non-robust P-DASH technique. The abbreviations, definitions and solution methods of the comparative schemes are summarized in Table II. Existing non-robust P-DASH techniques, referred to as *P-DASH*, are simulated by replacing the random rates in Eq. 1 with the average rate values. The performance bounds are obtained by *PP-DASH* which assumes perfect prediction of channel rates (without errors) to replace the random variable in C1 Eq. 1.

B. Evaluation Metrics

1) QoS Satisfaction and QoE Levels: In order to assess the robustness of the simulated schemes, we measure the QoS satisfaction using the number and duration of video stops

TABLE I
SUMMARY OF MODEL PARAMETERS

Parameter	Value
BS transmit power	43 dBm
Bandwidth	5 MHz
Time Horizon T	60 s
Streaming rates	$0.5, 1, 1.5, 2, 2.5$ [Mbps]
Bit Error Rate	5×10^{-5}
Shadow correlation distance(d_{cor}) [29]	$50m$
Shadow standard deviation [29]	$4, 6$
Velocity	25 - 40 [km/h]
Packet size	10^3 [bytes]
Packet rate (from core network to BS)	$10^3 s^{-1}$
Buffer size	10^9 [bits]

denoted by η and ζ, respectively and calculated as

$$\eta_i = \sum_{t=0}^{|\mathcal{T}|} \mathbb{1}_{R_{i,t} < D_{i,t}}. \tag{8}$$

$$\zeta_i = \int_0^{|\mathcal{T}|} \zeta_{i,\kappa} d\kappa / \int_0^{|\mathcal{T}|} d\kappa. \tag{9}$$

where $R_{i,t} = \sum_{t'=0}^{t} r_{i,t'} x_{i,t'}$ is the cumulative video content received by user i till time slot t while $r_{i,t}$ is the actual channel rate measured by user i at timeslot t. $\zeta_{i,\kappa}$ equals to 1 if user i experienced a video stop at time instant κ where $\kappa << t$. Both metrics are normalized to the total video duration and expressed in percentages.

While the network performance is calculated by the average of each QoS metric, the resultant Quality of Experience (QoE) is also reported to model the users' perception. QoE, in essence, is a subjective metric that represents the service end-to-end performance level from the user's perspective, and can be calculated using the Mean Opinion Score (MOS) formula in [31] and [32] depicted below:

$$MOS_{VS} = \frac{1}{|\mathcal{M}|} \sum_{i=1}^{|\mathcal{M}|} (2.99 \times e^{-0.96\eta_i} + 2.01). \tag{10}$$

$$MOS_{VD} = \frac{1}{|\mathcal{M}|} \sum_{i=1}^{|\mathcal{M}|} 4.59 \times e^{-3.44\zeta_i}. \tag{11}$$

Where MOS_{VS} and MOS_{VD} are the MOS values due to number and duration of video stops, respectively. The value of MOS varies from 1 to 5 which represents very poor to excellent service, respectively.

2) Video Streaming Quality: A key performance parameter of DASH is the selected quality of all the segments over the time horizon for each user i, denoted by V_i, and calculated as a function of the segment size as follows

$$V_i = \sum_{\forall t \in \mathcal{T}} \sum_{\forall q \in \mathcal{Q}_t} \kappa_{i,t}^{(q)} \upsilon_q \quad \forall i \in \mathcal{M} \tag{12}$$

The V_i metric is averaged over all users to assess the conservatism of the schemes, while the optimality of the objective function is measured by the fairness using the Jain's index below

$$J = \frac{(\sum_{i=1}^{|\mathcal{M}|} V_i)^2}{|\mathcal{M}| \sum_{i=1}^{|\mathcal{M}|} V_i^2} \tag{13}$$

C. Simulation Results

1) Comparison With Non-Robust P-DASH: We firstly compare both the SA and GA formulations of the introduced robust P-DASH against the existing *non-robust P-DASH* for different values of QoS degradations and standard deviations. The existing non-robust *P-DASH* suffered from an increased number and durations of video stops with the standard deviations of shadowing as depicted in Fig. 2(a) and Fig. 2(b), respectively. Although only four users are considered, this QoS degradation resulted in average and poor MOS values due to frequent stops with long durations as shown in Fig. 2(c) and Fig. 2(d), respectively. This is attributed to the average predicted values of rates adopted by the *P-DASH* which did not account for the rate variations and uncertainties. As such, the highest quality levels were always selected by the non-robust scheme as depicted in Fig. 3(a). This is as opposed to the introduced *GRP-DASH* and *SRP-DASH* formulations which were able to keep the percentage of stops and durations below the QoS degradation level $\epsilon \times 100\%$. An increasing trade-off between the QoS and QoE improvements on one hand and the quality degradation on the other hand is deduced over different ϵ levels as in Fig. 2(a)-Fig. 2(d) and Fig. 3(a), respectively. The main objective (i.e. quality fairness), did not suffer a significant degradation as reported by the Jain's index in Fig. 3(b).

By increasing the number of users, more and longer video stops are observed which resulted thus in low MOS values when using the *P-DASH* as shown in Fig. 4(a)-Fig. 4(d). This degradation is caused by the optimistic strategy of the *P-DASH* which tries to maximize the quality at the expense of pre-buffering and thus increases the chance of stops during channel variations. This was avoided by the *GRP-DASH* which, in essence, allocates more airtime than the *P-DASH* based on the standard deviation and the QoS degradation level ϵ. The optimality gap between the *P-DASH* and *RP-DASH* (GA and SA) also decreases with the increased load as shown in Fig. 5(a)-Fig. 5(b) since the former has to retroactively allocate extra airtime after detecting the video stops.

2) Gaussian and Scenario Based Comparisons: Comparing the *SRP-DASH* with *GRP-DASH*, the latter is found to be less robust, in terms of average stops, during the low standard deviations and high QoS degradation levels ϵ as shown in Fig. 2(a)-Fig. 2(b). However, this is not the case when the

TABLE II
COMPARATIVE SCHEMES

Notation	Definition	Solution Method
P-DASH	Existing non-robust P-DASH scheme in [9], [30]	Simplex or branch-and-cut methods in Gurobi [27].
PP-DASH	Hypothetical optimal P-DASH scheme with perfect channel knowledge	Simplex or branch-and-cut in Gurobi [27].
SRP-DASH	The proposed SA based RP-DASH as formulated in Eq. 3	Simplex or branch-and-cut in Gurobi [27].
GRP-DASH	The proposed GA based RP-DASH as formulated in Eq. 7	Simplex or branch-and-cut in Gurobi [27].
HRP-DASH	The proposed GA based RP-DASH as formulated in Eq. 7	Heuristic in Algorithm 1-2.

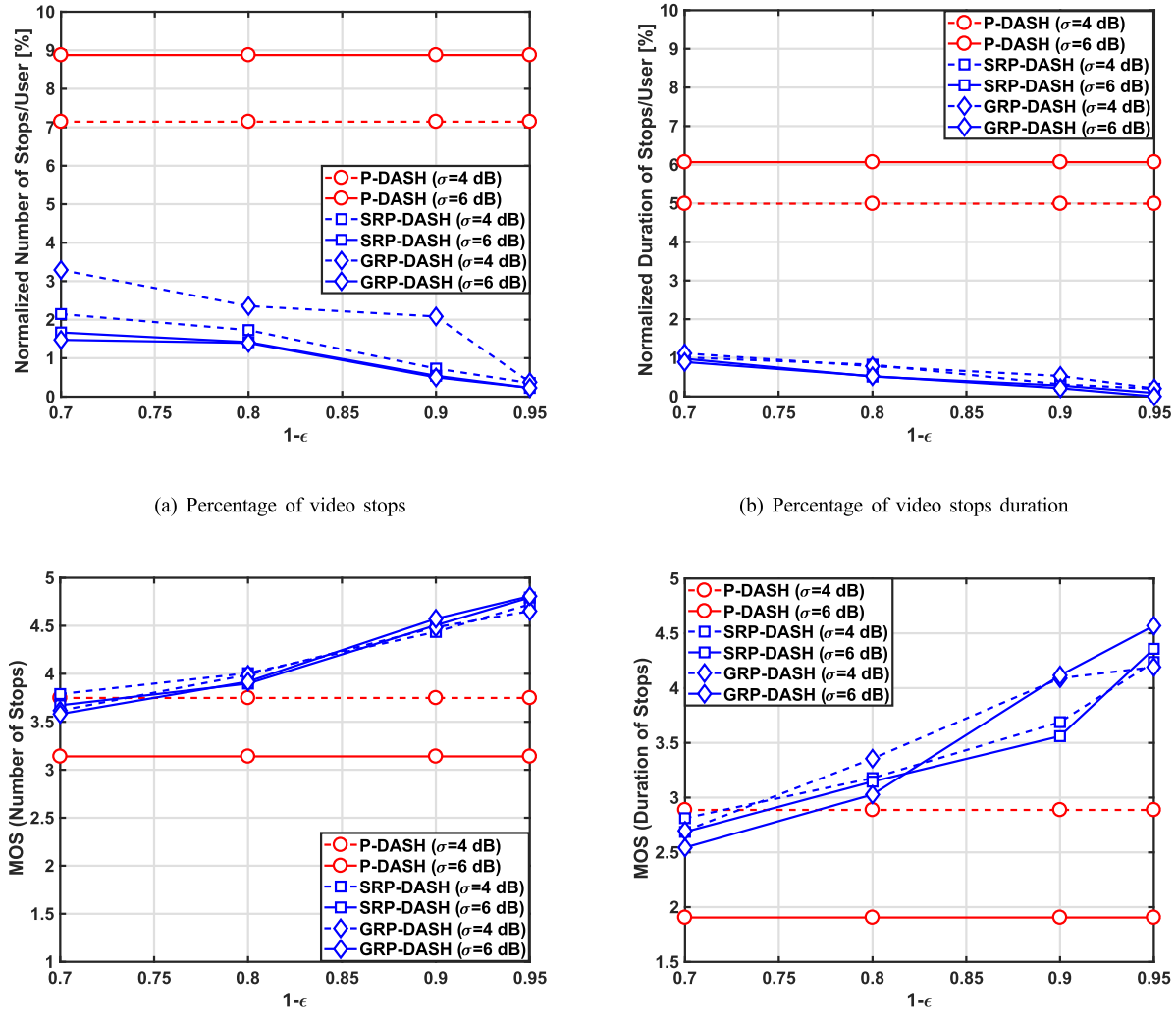

(a) Percentage of video stops

(b) Percentage of video stops duration

(c) Average MOS for the number of stops

(d) Average MOS for the stop durations

Fig. 2. QoS performance of RP-DASH (SA and GA) for 4 users at different degradation levels.

MOS is considered which illustrates that GA is equal or more robust than the SA as discussed in Section IV especially at very low values of ϵ. Since the MOS is calculated by an exponential function, it reveals that the GA provides a fair robustness across the users unlike the SA which decreases the average degradation and conservatism. The optimality gap in Fig. 3(a)-Fig. 3(b) reveals another trade-off between the amount of information, required by the SA, and the lower quality obtained by the GA.

3) Evaluation of the Heuristic and Complexity: The performance of the introduced heuristic is reported for different numbers of users in Fig. 4(a)-Fig. 4(d). Similar to the *GRP-DASH*, the *HRP-DASH* was able to satisfy the maximum QoS degradation level ϵ and provided a stable QoS performance

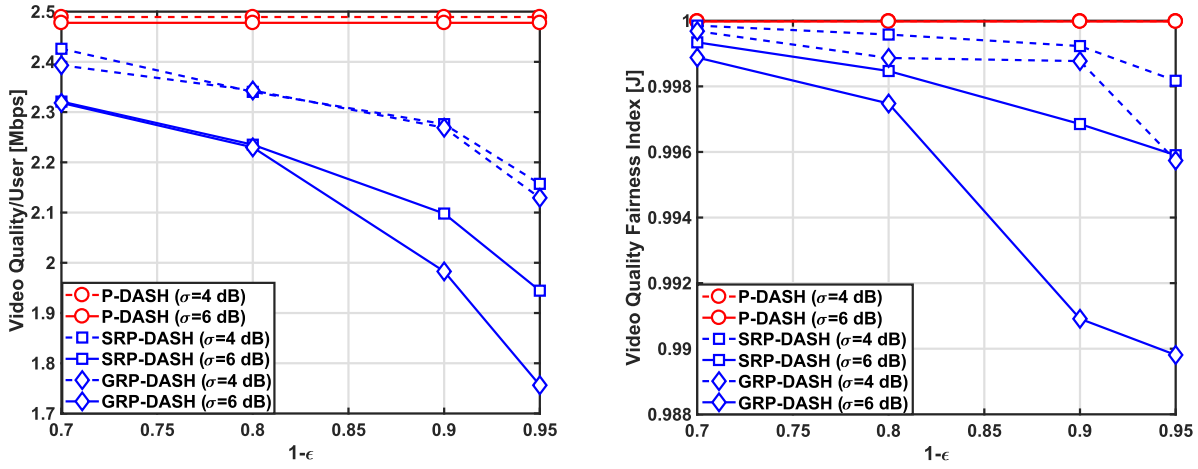

(a) Avergae video quality

(b) User quality fairness

Fig. 3. Quality performance of RP-DASH (SA and GA) for 4 users at different degradation levels.

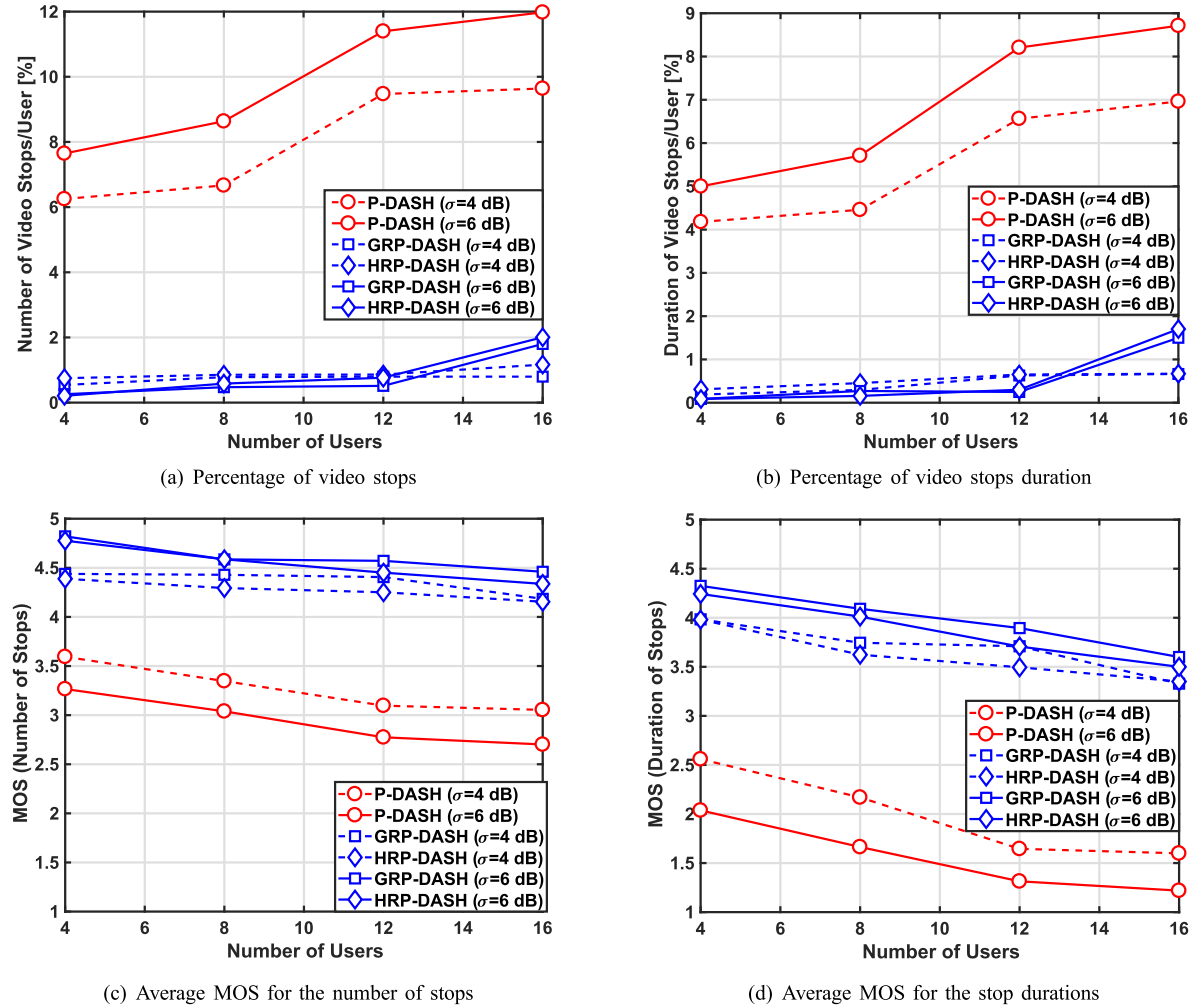

(a) Percentage of video stops

(b) Percentage of video stops duration

(c) Average MOS for the number of stops

(d) Average MOS for the stop durations

Fig. 4. QoS performance for different number of users at $\epsilon = 0.9$.

over the load and the channel standard deviation. It can be also seen that the *HRP-DASH* was slightly more conservative than the *GRP-DASH* and thus reported a smaller optimality gap in Fig. 5(a)-Fig. 5(b). This demonstrates the ability of the heuristic to exploit the problem structure and obtain near-optimal solutions that also satisfy the defined QoS degradation

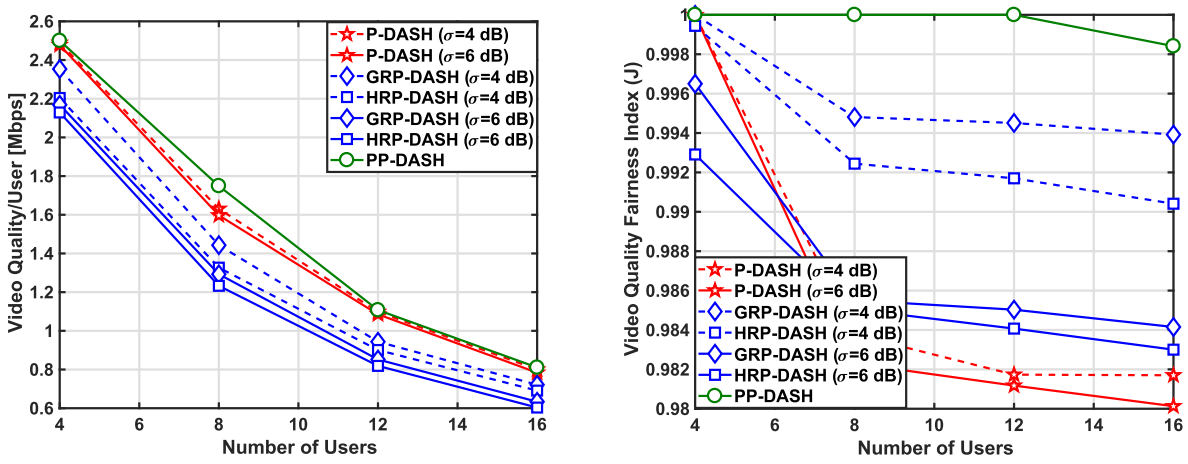

(a) Avergae video quality

(b) User quality fairness

Fig. 5. Quality performance for different number of users at $\epsilon = 0.9$.

TABLE III
EXECUTION TIME OF THE SIMULATED SCHEMES

Technique	Number of Users				QoS Degrad.	
	4	8	12	16	0.3	0.2
P-DASH	$50s.$	$120s.$	$290s.$	$600s.$	$30s.$	$30s.$
SRP-DASH	$60s.$	$200s.$	$320s.$	$600s.$	$50s.$	$55s.$
GRP-DASH	$50s.$	$120s.$	$260s.$	$560s.$	$30s.$	$40s.$
HRP-DASH	$<0.1ms.$	$<0.1ms.$	$<0.1ms.$	$<0.1ms.$	$<0.1ms.$	$<0.1ms.$

level ϵ. The complexity of the both optimal and heuristic techniques is measured in terms of the execution time as reported in Table III. The heuristic algorithm only requires less than 0.1 $ms.$ to solve the RP-DASH formulation irrespective of the network load (i.e. number of users) and the QoS degradation level ϵ. This is unlike the commercial solver which required tens or hundreds of seconds to reach the target duality gap. The execution time increases with both the number of users, due to the larger problem dimension, and the QoS level $(1-\epsilon)$ due to the tight feasibility region. When the optimal SA is used, more execution time is required compared to the GA due to the added auxiliary decision variables, thus, presenting a new trade-off between the complexity of SA and the conservatism of GA.

VIII. CONCLUSION

We introduced a *Robust Predictive*-DASH (RP-DASH) scheme to handle uncertainties in predicted rates while achieving streaming quality fairness among the users. The scheme adopts a stochastic formulation which incorporates the predicted information as random variables and guarantee the QoS satisfaction at a minimum probability level. Deterministic equivalent forms are then adopted to provide closed form solutions which can be solved either by commercial solvers for benchmark solutions, or by the proposed guided heuristic search for real-time decisions. The performance evaluation, using a standard compliant simulator, demonstrated the ability of probabilistic RP-DASH to satisfy the predefined QoS level. This is unlike the existing non-probabilistic P-DASH schemes which assume ideal prediction and thus experience increasing degradation in the users' QoS and QoE. The results further revealed a trade-off between the risk of experiencing video stops and maximizing video quality, which increases the need for a thorough modelling of user's preferences. As such, users seeking high video qualities should be assigned low QoS probabilistic levels (i.e. $1-\epsilon$) that compromise the number and duration of stops. In addition to satisfying the QoS level, the small optimality gap between the SA and GA promises the adoption of the latter in RP-DASH with quality maximization. This is unlike the existing conclusions on GA that doubted its robustness in long-term energy-efficient predictive video delivery. Adopting the GA in robust predictive DASH will decrease the cost of uncertainty modelling as the network operator will not rely on the exact realizations of future rates. Moreover, near-optimal real-time robust solutions are obtainable for the DASH scheme through a low complexity guided heuristic

algorithm that exploits the problem structure. All the above performance improvements and design flexibilities envision the implementation of RP-DASH in future wireless networks under practical uncertainties.

Our future work considers the following enhancements to the robust predictive DASH delivery:

1. Model the formulation using other user experience metrics such as the number and frequency of switching the quality. This enables assessing the performance gains and trade-offs of robust predictive DASH under different operator's and user's objectives.
2. Model the uncertainties in the channel vacant capacities which occurs in high dynamic scenarios with unexpected user arrivals. This ensures the QoS satisfaction for users requesting DASH and real-time applications.
3. Examine the potential of exploiting the user's selected quality to drive the P-DASH towards less conservative decisions. In particular, users selecting high-quality levels compared to the network based values can be used to learn the variance of the GA or the aggregated rate value of the SA. This provides real-time tracking of uncertainty level and adapts the degree of robustness.
4. Extend existing user experience models, i.e. QoE, to capture the trade-off between video stops and selected quality using the probabilistic metric. Particularly, a new QoE model is needed to consider the users preference, i.e. both quality and stops, as a function of the QoS level ϵ. Such model would guide the operator while selecting the value of ϵ jointly with the resources and quality of segments to reflect the user preference.
5. Existing P-DASH focused on optimizing either the QoS (e.g. video quality), in high load scenarios, or decreasing the energy-consumption in low load cases. A joint optimization model is desirable to autonomously evaluate the network load and select the best objective to optimize (e.g. energy or QoS parameter).

REFERENCES

[1] CISCO. (2015). *Cisco Visual Networking Index: Global Mobile Data Traffic Forecast Update, 2014–2019*. Accessed: Nov. 15, 2016. [Online]. Available: http://www.cisco.com/c/en/us/solutions/service-provider/visual-networking-index-vni/index.html

[2] T. Stockhammer, "Dynamic adaptive streaming over HTTP—Standards and design principles," in *Proc. 2nd Annu. ACM Conf. Multimedia Syst.*, 2011, pp. 133–144.

[3] M. Seufert, S. Egger, M. Slanina, T. Zinner, T. Hoßfeld, and P. Tran-Gia, "A survey on quality of experience of HTTP adaptive streaming," *IEEE Commun. Surveys Tuts.*, vol. 17, no. 1, pp. 469–492, 1st Quart., 2015.

[4] *Transparent End-to-End Packet-Switched Streaming Service (PSS); Progressive Download and Dynamic Adaptive Streaming Over HTTP (3GP-DASH)*, document TS 26.247 v10.7.0, 3GPP, 2012.

[5] A. El Essaili, D. Schroeder, E. Steinbach, D. Staehle, and M. Shehada, "QoE-based traffic and resource management for adaptive HTTP video delivery in LTE," *IEEE Trans. Circuits Syst. Video Technol.*, vol. 25, no. 6, pp. 988–1001, Jun. 2015.

[6] H. Abou-Zeid, H. S. Hassanein, and S. Valentin, "Energy-efficient adaptive video transmission: Exploiting rate predictions in wireless networks," *IEEE Trans. Veh. Technol.*, vol. 63, no. 5, pp. 2013–2026, Jun. 2014.

[7] Z. Lu and G. De Veciana, "Optimizing stored video delivery for mobile networks: The value of knowing the future," in *Proc. IEEE INFOCOM*, Apr. 2013, pp. 2706–2714.

[8] A. Schulman *et al.*, "Bartendr: A practical approach to energy-aware cellular data scheduling," in *Proc. ACM MobiCom*, 2010, pp. 85–96.

[9] R. Margolies *et al.*, "Exploiting mobility in proportional fair cellular scheduling: Measurements and algorithms," in *Proc. IEEE INFOCOM*, Apr./May 2014, pp. 1339–1347.

[10] X. K. Zou *et al.*, "Can accurate predictions improve video streaming in cellular networks?" in *Proc. 16th Int. Workshop Mobile Comput. Syst. Appl.*, 2015, pp. 57–62.

[11] H. Abou-Zeid, H. S. Hassanein, Z. Tanveer, and N. A. Ali, "Evaluating mobile signal and location predictability along public transportation routes," in *Proc. IEEE WCNC*, Mar. 2015, pp. 1195–1200.

[12] N. Bui, F. Michelinakis, and J. Widmer, "A model for throughput prediction for mobile users," in *Proc. Eur. Wireless*, May 2014, pp. 1–6.

[13] R. Atawia, H. Abou-Zeid, H. S. Hassanein, and A. Noureldin, "Robust resource allocation for predictive video streaming under channel uncertainty," in *Proc. IEEE GLOBECOM*, Dec. 2014, pp. 4683–4688.

[14] R. Atawia, H. Abou-Zeid, H. S. Hassanein, and A. Noureldin, "Chance-constrained QoS satisfaction for predictive video streaming," in *Proc. IEEE LCN*, Oct. 2015, pp. 253–260.

[15] R. Atawia, H. Abou-Zeid, H. S. Hassanein, and A. Noureldin, "Joint chance-constrained predictive resource allocation for energy-efficient video streaming," *IEEE J. Sel. Areas Commun.*, vol. 34, no. 5, pp. 1389–1404, May 2016.

[16] S. Cicalò, N. Changuel, V. Tralli, B. Sayadi, F. Faucheux, and S. Kerboeuf, "Improving QoE and fairness in HTTP adaptive streaming over LTE network," *IEEE Trans. Circuits Syst. Video Technol.*, vol. 26, no. 12, pp. 2284–2298, Dec. 2016.

[17] K. J. Ma and R. Bartos, "HTTP live streaming bandwidth management using intelligent segment selection," in *Proc. IEEE Global Telecommun. Conf. (GLOBECOM)*, Dec. 2011, pp. 1–5.

[18] P. Georgopoulos, Y. Elkhatib, M. Broadbent, M. Mu, and N. Race, "Towards network-wide QoE fairness using openflow-assisted adaptive video streaming," in *Proc. ACM SIGCOMM Workshop Future Human-Centric Multimedia Netw.*, 2013, pp. 15–20.

[19] A. Seetharam, P. Dutta, V. Arya, J. Kurose, M. Chetlur, and S. Kalyanaraman, "On managing quality of experience of multiple video streams in wireless networks," *IEEE Trans. Mobile Comput.*, vol. 14, no. 3, pp. 619–631, Mar. 2015.

[20] N. Bui and J. Widmer, "Modelling throughput prediction errors as Gaussian random walks," in *Proc. KuVS Workshop Anticipatory Netw.*, 2014, pp. 1–3.

[21] R. Ramamonjison and V. K. Bhargava, "Sum energy-efficiency maximization for cognitive uplink networks with imperfect CSI," in *Proc. IEEE WCNC*, Apr. 2014, pp. 1012–1017.

[22] N. Y. Soltani, S.-J. Kim, and G. B. Giannakis, "Chance-constrained optimization of OFDMA cognitive radio uplinks," *IEEE Trans. Wireless Commun.*, vol. 12, no. 3, pp. 1098–1107, Mar. 2013.

[23] M. J. Abdel-Rahman and M. Krunz, "Stochastic guard-band-aware channel assignment with bonding and aggregation for DSA networks," *IEEE Trans. Wireless Commun.*, vol. 14, no. 7, pp. 3888–3898, Jul. 2015.

[24] P. Kali and S. W. Wallace, *Stochastic Programming*. New York, NY, USA: Springer, 1994.

[25] J. Yao, S. S. Kanhere, and M. Hassan, "Improving QoS in high-speed mobility using bandwidth maps," *IEEE Trans. Mobile Comput.*, vol. 11, no. 4, pp. 603–617, Apr. 2012.

[26] W. W.-L. Li, Y. J. Zhang, A. M.-C. So, and M. Z. Win, "Slow adaptive OFDMA systems through chance constrained programming," *IEEE Trans. Signal Process.*, vol. 58, no. 7, pp. 3858–3869, Jul. 2010.

[27] Gurobi. *Gurobi Optimization*. Accessed: Mar. 29, 2017. [Online]. Available: http://www.gurobi.com/

[28] G. Piro, N. Baldo, and M. Miozzo, "An LTE module for the ns-3 network simulator," in *Proc. Int. ICST Conf. Simulation Tools Techn.*, 2011, pp. 415–422.

[29] "LTE; Evolved universal terrestrial radio access (E-UTRA); further advancements for E-UTRA physical layer aspects," 3GPP, Tech. Rep. TR 36.814 V9.0.0, 2010.

[30] H. Abou-Zeid, H. S. Hassanein, and N. Zorba, "Long-term fairness in multi-cell networks using rate predictions," in *Proc. IEEE GCC Conf. Exhibit. (GCC)*, Nov. 2013, pp. 131–135.

[31] T. Hoßfeld, M. Seufert, M. Hirth, T. Zinner, P. Tran-Gia, and R. Schatz, "Quantification of Youtube QoE via crowdsourcing," in *Proc. IEEE Int. Symp. Multimedia (ISM)*, Dec. 2011, pp. 494–499.

[32] L. G. M. Ballesteros, S. Ickin, M. Fiedler, J. Markendahl, K. Tollmar, and K. Wac, "Energy saving approaches for video streaming on smartphone based on QoE modeling," in *Proc. 13th IEEE Annu. Consum. Commun. Netw. Conf. (CCNC)*, Jan. 2016, pp. 103–106.

Ramy Atawia (S'12–M'17) received the B.Sc. and M.Sc. degrees in communication engineering from German University in Cairo, Egypt, in 2012 and 2013, respectively, and the Ph.D. degree in electrical and computer engineering from Queen's University in 2017. He was a Member of Technical Staff and a Researcher with Bell Laboratories, and Nokia, Belgium. He was with Vodafone working on automating the design and optimization of radio networks, and with Nokia focusing on customer experience management and analytics. He was a Teaching Assistant and a Guest Lecturer, where he delivered tutorials on optimization, wireless networks, and programming. He is currently an Indoor Radio Solutions Developer at Ericsson Research and Development, Canada. His research work appeared in top-tier IEEE journals and conferences, and led to 15 patents. His research interests include stochastic optimization, predictive video streaming, machine learning, and the AI driven management of indoor networks. He also serves as a TPC member and a reviewer in IEEE flagship conferences and journals. He was a recipient of the Best Paper Award at the IEEE GLOBECOM 2017.

Hossam S. Hassanein (S'86–M'90–SM'05–F'17) is a leading authority in the areas of broadband, wireless and mobile networks architecture, protocols, control, and performance evaluation. His record spans over 500 publications in journals, conferences, and book chapters, in addition to numerous keynotes and plenary talks in flagship venues. He has received several recognitions and best papers awards at top international conferences. He is also the Founder and the Director of the Telecommunications Research Laboratory, Queen's University School of Computing, with extensive international academic and industrial collaborations. He is a Former Chair of the IEEE Communication Society Technical Committee on Ad hoc and Sensor Networks. He is an IEEE Communications Society Distinguished Speaker (Distinguished Lecturer 2008–2010).

Aboelmagd Noureldin (S'98–M'02–SM'08) received the B.Sc. degree in electrical engineering and the M.Sc. degree in engineering physics from Cairo University, Egypt, in 1993 and 1997, respectively, and the Ph.D. degree in electrical and computer engineering from the University of Calgary, Calgary, AB, Canada, in 2002. He is currently a Professor at the Department of Electrical and Computer Engineering, Royal Military College of Canada (RMCC) with a cross-appointment at the School of Computing and the Department of Electrical and Computer Engineering, Queen's University. He is also the Founder and the Director of the Navigation and Instrumentation Research Group, RMCC. He has authored or co-authored over 230 papers in journals and conference proceedings. His research work led to ten patents in the area of position, location, and navigation systems. His research is related to GPS, wireless location and navigation, indoor positioning, and multi-sensor fusion.